LETTER TO THE EDITOR

Simultaneous analysis of changes in long-range and short-range structural order at the displacive phase transition in quartz

Matthew G Tucker†, Martin T Dove†§ and David A Keen‡

† Mineral Physics Group, Department of Earth Sciences, University of Cambridge, Downing Street, Cambridge, CB2 3EQ, UK
‡ ISIS Facility, Rutherford Appleton Laboratory, Chilton, Didcot, Oxfordshire, OX11 0QX, UK

E-mail: `mtuc98@esc.cam.ac.uk` (M G Tucker) `martin@esc.cam.ac.uk` (M T Dove) and `d.a.keen@rl.ac.uk` (D A Keen)

Abstract. A new look at the displacive phase transition in quartz is reported, using neutron total diffraction experiments and a new implementation of the Reverse Monte Carlo method in which explicit account is taken of the Bragg peak intensities. This approach yields information about short-range and long-range details of the phase transition simultaneously, and reproduces both aspects of the structure correctly and self-consistently. This study gives, for the first time, a visualization of what actually happens at the phase transition. The picture which emerges is that the symmetry-change associated with the phase transition allows the excitation of many low-frequency high-amplitude modes of vibration which create considerable orientational disorder of the SiO_4 tetrahedra.

1. Introduction

The displacive phase transition in quartz (SiO_2) at $T_c = 846$ K has been the subject of so many studies over the past 100 years [1, 2] that it is surprising that there is still no firm picture of what actually happens at the phase transition. Moreover, the question of what actually happens at any displacive phase transition is often controversial, because most studies, whether experimental or theoretical, tend to focus on either the long-range order or the short-range order separately, rather than considering them *simultaneously*. In brief, the different perspectives polarize into two extremes. One is the classical soft-mode picture, in which the atoms vibrate around mean positions which change (through symmetry-breaking displacements) on cooling through T_c, and the displacive mode acts as the classical soft mode. In the other extreme, the structure of the high-symmetry phase has the atoms hopping between the positions corresponding to the different domains of the low-symmetry phase, so that there is dynamic disorder in the high-symmetry phase, and on cooling the atoms progressively occupy the positions corresponding to one domain in the low-symmetry phase. Both extremes have been argued for the displacive phase transition in quartz [2]. In particular for quartz, although a soft mode is observed on heating up to T_c, it becomes heavily damped on passing though T_c [3]. In standard models this can arise when the picture is somewhere between the two extremes, that is, when the

§ To whom correspondence should be addressed.

displacive phase transition has some character of order–disorder. This letter shows that the situation is actually not so simply rationalized. Using new analysis methods applied to neutron diffraction experiments on quartz, we are able to suggest that the phase transition also involves new low-energy high-amplitude vibrations that are excited as a result of the phase transition. These create a disordered state, but only in a way that does not lend itself to an interpretation in terms of order–disorder or domain models. The changes in the structural disorder associated with the phase transition are distinct from the effects of normal critical fluctuations and from the structural changes associated with the incommensurate modulation that exists for ~ 1.5 K around the α–β transition. Instead, we suggest that the disorder arises from new low-energy modes that are excited only in the high-temperature phase.

2. Methods

The work we discuss here involves measurements of the total neutron powder diffraction from quartz, $S(Q)$, which includes both the Bragg and diffuse scattering, over a wide range of temperatures encompassing the phase transition. From the Bragg scattering data and the Fourier transform of the total diffraction we can obtain information about the long-range and short-range order respectively. The use of large values of the scattering vector Q, made possible using time-of-flight neutron diffraction, ensures that we can obtain good resolution (equal to $2\pi/Q_{max}$) in real space, essential if the data are to be used to differentiate between different interpretations of the structural aspects of the phase transition and of the high-temperature phase. The *novel feature of our work* is to combine both sets of data to perform constrained reverse Monte Carlo (RMC) refinements [4]. The explicit use of the Bragg intensities ensures that the RMC refinement gives configurations that have the correct long-range 'average' structure and symmetry, and avoids any exaggeration of the structural disorder. This work has enabled us to correlate changes in the short-range structure with the onset of long-range changes in the structure, and to visualize, for the first time, the changes in the structure through the phase transition.

The total neutron powder diffraction data were obtained on the LAD diffractometer at the ISIS pulsed neutron source. The sample was a finely-ground powder of natural quartz, contained in an 8 mm diameter vanadium can. The sample was mounted into either a closed-cycle helium refrigerator or vanadium foil neutron furnace for low- or high-temperature measurements respectively. Data were collected for a range of temperatures between 20–1073 K. Standard corrections for the $S(Q)$ data were applied [5]. The final $S(Q)$ functions extended across the range 0.2–40 Å^{-1}.

Rietveld refinements of the crystal structure were carried out at each temperature using the higher-resolution data from the back-scattering detectors to obtain the 'average' structure and accurate lattice parameters. The Pawley method [6] was used to extract corrected Bragg intensities for use in the RMC refinements. The total pair correlation functions $T(r)$ were obtained by an inverse Fourier transform method [7]. The RMC refinements were based on the protocols developed by Keen [4]. These use slack constraints on the Si–O bond length (obtained from the $T(r)$ data) and the tetrahedral O–Si–O angles primarily in order to maintain the network connectivity rather than to ensure correct interatomic distances within the tetrahedra *per se*. The RMC refinement fitted both the reciprocal $S(Q)$ and real-space $T(r)$ data, and the intensities of the Bragg peaks all at the same time. This is the first time that the RMC method has been used in this way. Orthorhombic configurations representing the trigonal α-(low) quartz and hexagonal β-(high) quartz structure were used in the RMC modelling, starting with atom positions determined from the Rietveld refined structural parameters at each temperature. Each configuration contained $10 \times 10 \times 10$ (orthorhombic) unit cells and 18 000 atoms. We will flag a number of internal consistency checks below that point to the reliability of our methods.

3. Results

Figure 1 shows total pair correlation functions $T(r)$ from quartz for a wide range of temperatures. The development of structural disorder, seen as the loss of sharpness in the features in $T(r)$, is gradual and increases continuously with increasing temperature — the $\alpha–\beta$ phase transition is not immediately obvious in the broadening features in $T(r)$. However, the positions of high-r peaks (such as those marked at $\sim$ 17 Å in figure 1) shift in an identical manner to the linear thermal expansion of quartz, which does show a change at T_c (this is one of our consistency checks). In figure 2(a) the comparison is highlighted by plotting the temperature dependence of the cube of the peak position (suitably scaled) with the temperature dependence of the unit cell volume, and it can be seen that there is a very good match. On the other hand, the local SiO_4 tetrahedral units, defined by the Si–O bond length at $\sim$ 1.6 Å and the O–O distance at $\sim$ 2.6 Å, do not show the same expansion, but neither do they show the apparent Si–O bond contraction seen in the average structure (figure 2(b)). These two low-r peaks in $T(r)$ give a direct model-independent measure of the SiO_4 tetrahedral expansion, which is similar to that in cristobalite and continuous through T_c.
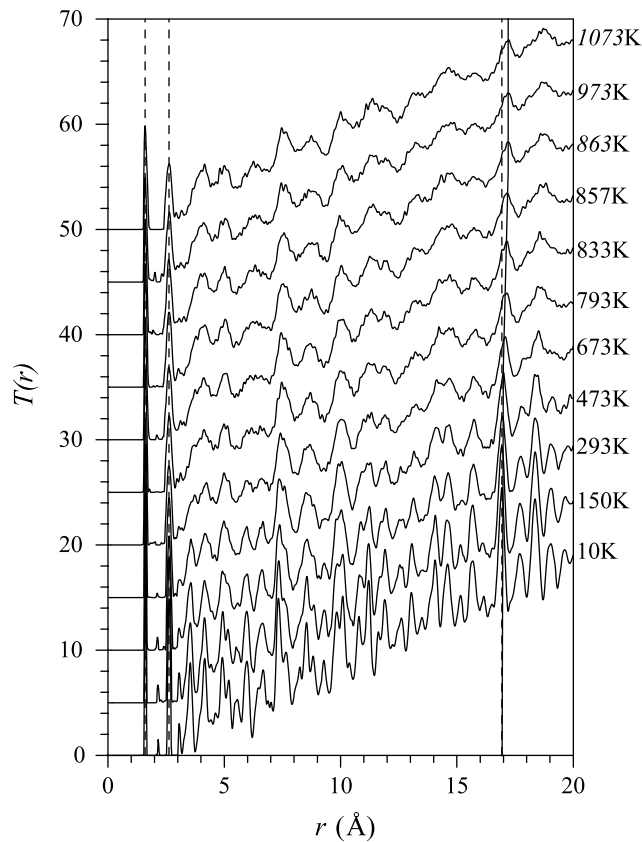
Figure 1. Neutron $T(r)$ functions of quartz over a wide range of temperatures. The dashed lines through the two lowest-r peaks follow the temperature evolution of the Si–O and O–O bond distances, and the full line through the peak at around 17 Å follows an interatomic distance that scales with the average linear thermal expansion. There is a progressive error on our temperature measurements; the nominal measurement of 858 K corresponds to the phase transition.
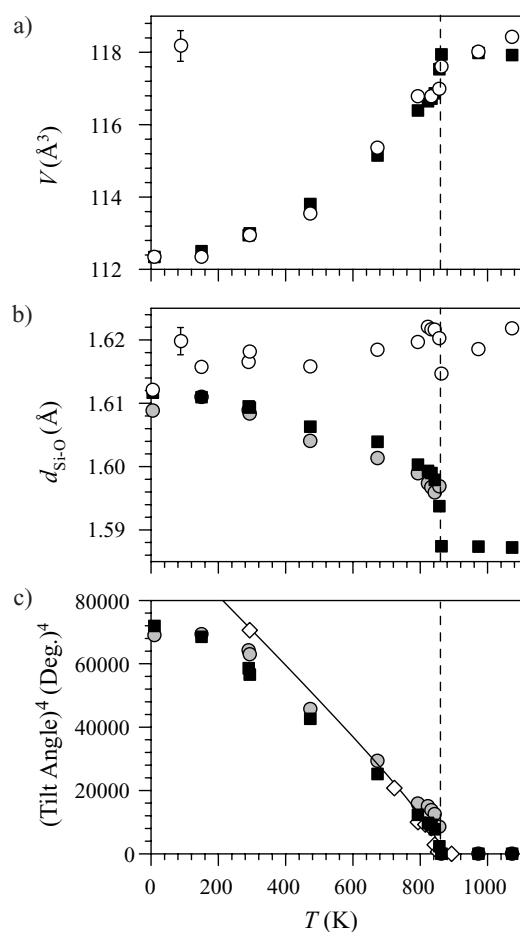
Figure 2. Temperature dependence of the (a) unit cell volume, (b) Si–O distance, and (c) fourth power of the average SiO_4 tetrahedral tilt angle. The vertical dashed line shows T_c. In (a) data from the Rietveld refinement and the 17 Å peak in $T(r)$ are given by squares and open circles respectively. In (b) squares and filled circles represent the distances between average positions, $\langle Si \rangle - \langle O \rangle$ given by Rietveld refinement and the RMC respectively, and the open circles represent the average values of the instantaneous bond length, $\langle Si–O \rangle$ from RMC. In (c) squares and filled circles represent data from Rietveld refinements and RMC respectively, and diamonds and line represent experimental x-ray diffraction data and results of a fitted Landau free-energy function [8]. In (a) and (b) we show the maximum non-sytemmatic errors on one set of data by drawing an error bar in the top left corner of each plot; in all other cases the non-sytemmatic errors are smaller than the sizes of the points.

The distances between average Si and O positions, $\langle Si \rangle - \langle O \rangle$, as determined from Rietveld refinement and the RMC configurations are compared with the average instantaneous Si–O distance, $\langle Si–O \rangle$, in figure 2(b). The important consistency check is that $\langle Si–O \rangle \rightarrow \langle Si \rangle - \langle O \rangle$ as $T \rightarrow 0$ and thermal fluctuations are reduced.

The order parameter for the displacive phase transition in quartz is given by the angle each SiO_4 tetrahedron rotates about the hexagonal or trigonal 100 directions. This can be calculated directly from the average atom positions $\langle Si \rangle$ and $\langle O \rangle$. The results from both the Rietveld refinements and RMC models are shown in figure 2(c). The

agreement between the two sets of results gives another of our consistency checks, as also is the agreement with earlier x-ray diffraction and Landau fits [8].

Sections from three configurations are shown in figure 3, together with the average structure extracted from them. The average structures match the crystallographic structures of α- and β-quartz exactly. The configuration at 1073 K (β-quartz) clearly *does not consist of domains*, but of smoothly varying tetrahedral orientational disorder. The model at 793 K (α-quartz) shows considerable orientational disorder, even though it is below T_c, whereas the model at 20 K remains ordered.
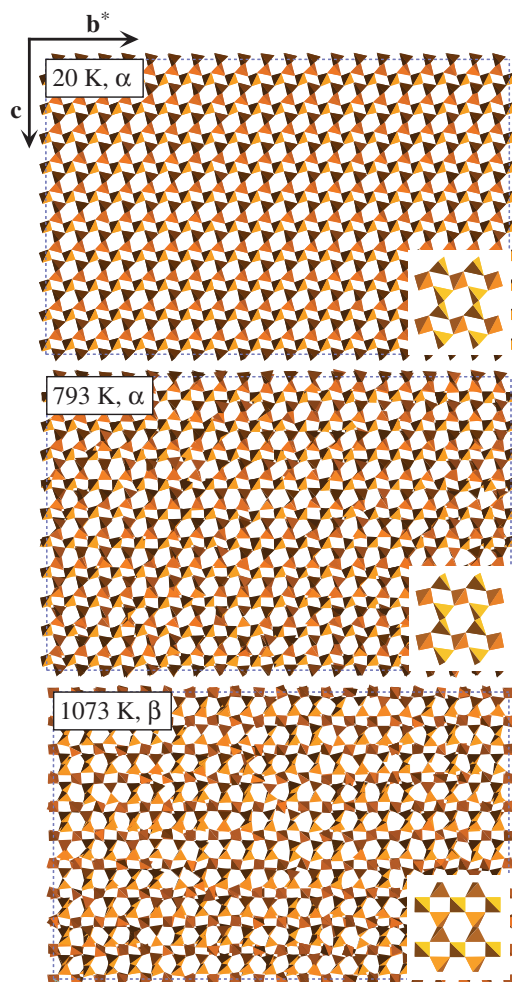
Figure 3. (100) layers of instantaneous RMC atomic configurations of quartz represented by SiO_4 tetrahedra for one temperature above T_c and two below. The inserts show the "average" structures obtained from the same configurations. In this projection the small parallelopiped gaps between tetrahedra become orthogonal in the β-phase, giving a clear representation of the symmetry change at T_c.

Figure 4 shows the distribution of nearest-neighbour Si–Si–Si angles at several temperatures and the temperature-dependence of the positions and widths of two peaks in the distribution which coalesce above T_c. This is a short-range correlation (the Si–Si distance

is ~ 3 Å), but the merging of the two peaks as a result of the phase transition indicates that some aspects of the short-range structure reflect the changes in the long-range order. However, the widths of the peaks in the distribution increase linearly with temperature and are not sensitive to the phase transition. The fact that the phase transition is clearly reflected in the temperature-dependence of positions of the peaks in the Si–Si–Si angle distribution is conclusive evidence against 'domain' theories of this phase transition.
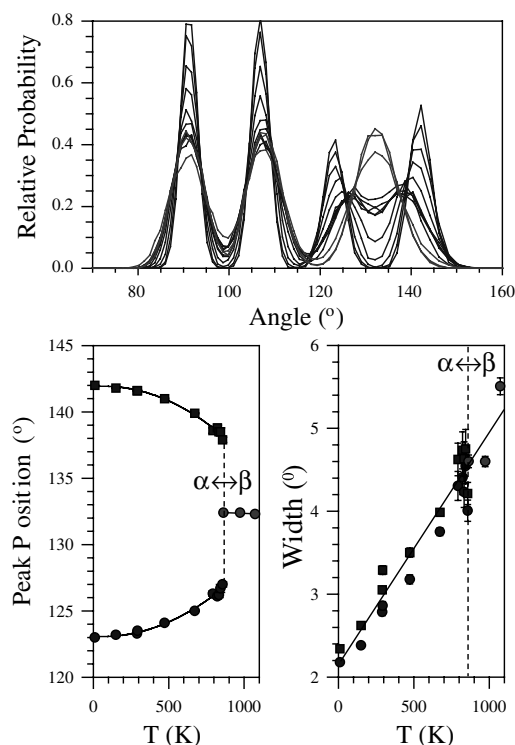
Figure 4. The upper plot shows the nearest-neighbour Si–Si–Si angle distribution in quartz. The lower two plots show the temperature-dependence of the positions and widths of the two peaks that coalesce in the β phase. In the angle distribution, the tempeartures are the same as those in figure 1, with the lowest temperature corresponding to the peaks with higher maximum values and the highest temperature corresponding to the peaks with the lowest maximum values.

4. Discussion

We now return to the general discussion raised in the introduction, and consider how the main points highlighted from the experimental data above facilitate a clear understanding of what actually happens at the displacive phase transition. In effect we have, for the first time, obtained an instantaneous 'visualization' of the phase transition at an atomic level. The data we have presented clearly show that the structure of the high-temperature phase does not consist of domains of an ordered structure, and does not involve the SiO_4 tetrahedra jumping between two orientations as in a classical order–disorder phase transition. But we also see that there is considerable orientational disorder that sets in at temperatures well below T_c and continues to increase on heating through T_c. There are clearly aspects of the short-range structure that are

completely insensitive to the phase transition, such as the actual Si–O bond length, but other aspects that are affected by the phase transition, such as the distribution of Si–Si–Si angles.

The picture that emerges from our analysis is that there is much more thermally-induced dynamic disorder than in either the classical soft-mode or domain models outlined in the introductory paragraph, and this disorder sets in at temperatures considerably below T_c. Where this disorder comes from can be understood from the 'rigid unit mode' (RUM) model [9–11]. In this model, the RUMs are phonon modes in which the SiO_4 tetrahedra are able to move as rigid objects without distorting significantly, and hence RUMs are the vibrations with the lowest frequencies. Low frequencies lead to large amplitudes, and this means that the large-amplitude rotations and displacements of the tetrahedra as seen in the β-phase configuration in figure 3 are primarily due to the excitation of RUMs. Detailed calculations have shown that there are significantly more RUMs in the β-phase than in the α-phase, and the frequencies of the modes that are RUMs only in the β-phase will increase rapidly on cooling below T_c [10]. The soft mode for the displacive phase transition is a RUM in the β-phase. The evident orientational disorder in the β-phase is due to the excitation of the soft mode and all the other RUMs. The increase in disorder in the α-phase on heating is due to the increasing amplitude of the modes that will become RUMs in the β-phase as their frequencies decrease. Calculations of the diffuse scattering from our RMC configurations show features that are consistent with the predictions of the RUM model, and which are also in quantitative agreement with our own single-crystal diffuse neutron scattering (to be published) in both the reciprocal space distribution and its temperature dependence. This is yet another consistency check on the methods used in this letter. The large number of RUMs that are active in the β-phase means that there is no need for the system to form domains in order to preserve the integrity of the SiO_4 tetrahedra. Thus we have a final picture of the dynamics of the phase transition which is more like the soft-mode model, except that the change in symmetry at the phase transition allows the excitation of a large number of low-frequency high-amplitude RUMs which in turn allow the formation of considerable orientational disorder.

In summary, the use of total neutron diffraction data and RMC modelling methods have given a new visualization of the displacive phase transition in quartz and allowed a direct comparison of changes in the structure at both the local and long-range level. The data have shown how different aspects of the structure may or may not be sensitive to the phase transition. The important finding is that there is considerable dynamic disorder that sets in at the phase transition, not due to the fluctuations of the order parameter *per se*, as in critical fluctuations, but to the excitation of new low-energy vibrations that are allowed to be excited as a result of the symmetry change associated with the phase transition. It is clear that any domain model of the high-temperature phase that supposes that the SiO_4 tetrahedra are flipping between well-defined orientations is completely inappropriate. But we also see why the soft mode is overdamped, not because of some degree of an order–disorder nature of the phase transition, but because the phase transition has allowed the excitation of many new low-energy high-amplitude vibrations that are able to couple through anharmonic interactions with the soft mode.

We have relied on a new implementation of the RMC method that uses the intensities of Bragg peaks explicitly. This has ensured that the RMC configurations are consistent with experimental data in both the short-range and long-range structural detail. A number of internal consistency checks have given us confidence in our structural models and demonstrated the effectiveness of the methods in producing configurations that are quantitatively representative of the short- and long-range structure simultaneously.

References

[1] Dolino G 1990 *Phase Transitions* **21** 59
[2] Heaney P J 1994 *Rev. in Mineral. & Geochem.* **29** 1
[3] Dolino G, Berge B, Vallade M and Moussa F 1992 *J. Physique. I* **2** 1461
[4] Keen D A 1997 *Phase Transitions* **61** 109
[5] Howe M A, McGreevy R L and Howells W S 1989 *J. Phys.: Condens. Matter* **1** 3433
[6] Pawley G S 1981 *J. Appl. Crys.* **14** 357
[7] Pusztai L and McGreevy R L 1997 *Physica B* **234–6** 357
[8] Grimm H and Dorner B 1975 *J. Phys. Chem. Sol.* **36** 407
[9] Bethke J, Dolino G, Eckold G, Berge B, Vallade M, Zeyen C M E, Hahn T, Arnold H and Moussa F 1987
        Europhys. Lett. **3** 601
[10] Hammonds K D, Dove M T, Giddy A P, Heine V and Winkler B 1996 *Am. Min.* **81** 1057
[11] Dove M T, Trachenko K O, Tucker M G and Keen D A 2000 *Rev. in Mineral. & Geochem.* **39** 1